

Spatio-Temporal Graph Contrastive Learning

Xu Liu^{*1}, Yuxuan Liang^{*1}, Yu Zheng², Bryan Hooi¹, Roger Zimmermann¹

¹School of Computing, National University of Singapore, Singapore

²JD iCity & JD Intelligent Cities Research, JD Tech, Beijing, China

{liuxu, yuxliang, bhooi, rogerz}@comp.nus.edu.sg; msyuzheng@outlook.com

Abstract

Deep learning models are modern tools for spatio-temporal graph (STG) forecasting. Despite their effectiveness, they require large-scale datasets to achieve better performance and are vulnerable to noise perturbation. To alleviate these limitations, an intuitive idea is to use the popular data augmentation and contrastive learning techniques. However, existing graph contrastive learning methods cannot be directly applied to STG forecasting due to three reasons. First, we empirically discover that the forecasting task is unable to benefit from the pretrained representations derived from contrastive learning. Second, data augmentations that are used for defeating noise are less explored for STG data. Third, the semantic similarity of samples has been overlooked. In this paper, we propose a Spatio-Temporal Graph Contrastive Learning framework (STGCL) to tackle these issues. Specifically, we improve the performance by integrating the forecasting loss with an auxiliary contrastive loss rather than using a pre-trained paradigm. We elaborate on four types of data augmentations, which disturb data in terms of graph structure, time domain, and frequency domain. We also extend the classic contrastive loss through a rule-based strategy that filters out the most semantically similar negatives. Our framework is evaluated across three real-world datasets and four state-of-the-art models. The consistent improvements demonstrate that STGCL can be used as an off-the-shelf plug-in for existing deep models.

1 Introduction

Deploying a large number of sensors to perceive an urban environment is the basis for building a smart city. The time-varying data that are produced from the distributed sensors can usually be represented as spatio-temporal graphs (STG). Leveraging the generated data, one important task is to forecast future trends based on historical observations. The state of the art to this problem can be categorized into convolutional neural networks (CNN) (Wu et al. 2019; Li and Zhu 2021) or recurrent neural networks (RNN)-based methods (Pan et al. 2019; Bai et al. 2020), depending on their techniques for modeling temporal correlations. For capturing the spatial correlations, these methods mainly use the popular Graph Neural Networks (GNN) (Kipf and Welling 2017; Veličković et al. 2018).

Recently, a series of contrastive learning-based methods on graphs have been proposed, and have achieved outstanding performance on several tasks in unsupervised settings (Velickovic et al. 2019; Hu et al. 2020; You et al. 2020). The common idea of these approaches is to maximize agreement between representations of graph elements with similar semantics (positive pairs), while minimizing those with unrelated semantic information (negative pairs). For the works that apply data augmentations (You et al. 2020; Zhu et al. 2021), positive pairs are obtained by applying graph data augmentations to generate two views of the same graph (termed *anchor*), and negative pairs are formed between the anchor and other graphs' views within a batch. In this way, generalizable and robust representations can be obtained.

In this work, we aim to enhance STG forecasting with an auxiliary contrastive learning task. The reasons lie in two aspects. Firstly, publicly available datasets in this area usually possess only a few months of data, which limits the number of training samples that can be built. Secondly, the sensor readings are never perfectly accurate or sometimes missing due to some unexpected factors, such as signal interruption (Yi et al. 2016). By using data augmentations and training the model with a supplementary contrastive loss, we are able to provide additional supervision signals and learn quality representations that are invariant to disturbance. However, existing graph contrastive learning methods (e.g. GraphCL (You et al. 2020)) cannot be directly applied to STG forecasting due to the following challenges.

- *Two-stage training procedure.* According to the typical two-stage training procedure in graph representation learning, we can first train a spatio-temporal encoder with a contrastive objective and then linearly evaluate or fine-tune the encoder with an untrained decoder to predict the future. However, we empirically find that both two-stage approaches perform worse than the purely supervised approaches in Figure 1. The results indicate that the pretrained representations learned from contrastive objective have few benefits to the forecasting task, which is different from the situation in using node/graph classifications as downstream tasks (You et al. 2020).
- *Less-explored data augmentation.* Data augmentations play an important role in contrastive learning methods (Chen et al. 2020). They help the model to learn invariant representations under different types and levels of pertur-

^{*}These authors contributed equally.

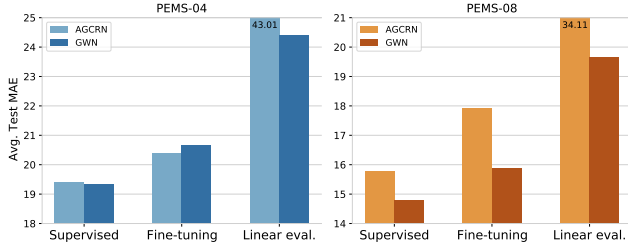


Figure 1: Prediction errors on PEMS-04/08 (Guo et al. 2019) by using AGCRN (Bai et al. 2020) and GWN (Wu et al. 2019) as base models. The *Supervised* bar indicates the normal procedure (end-to-end) of the forecasting task, while the others contain two stages. See more details in Appendix.

bations. However, so far data augmentations have been less explored for STG. For example, the intrinsic properties of STG data (especially temporal dependencies) are not utilized in current graph augmentation methods.

- *Ignoring sample’s semantic similarity.* In recent graph contrastive methods, all the other samples within a batch are seen as negative samples for a given anchor. This may not be reasonable in STG, since the samples in STG forecasting have inherent relationships to each other, such as closeness and periodic patterns (Zhang, Zheng, and Qi 2017). Figure 4 shows an example: the sample (pattern) from 6 am to 7 am on Monday is very similar to the same time period on Tuesday, which indicates the periodicity. In this case, it is not suitable to set these two semantically similar samples as a negative pair, i.e., no need to push apart their representations. Thus, we need an approach that can effectively identify negative samples.

To tackle the foregoing challenges, in this paper, we propose a novel framework named Spatio-Temporal Graph Contrastive Learning (STGCL). Three major adaptations are made to the existing graph contrastive paradigm based on the unique properties of STG. Primarily, we enhance the model performance by coupling the original forecasting loss with a contrastive loss instead of relying on two separate stages. Moreover, for constructing a positive pair, we design four types of augmentation methods that perturb the input data in three aspects: graph structure, time domain, and frequency domain. In addition, regarding the negative pairs, we devise a rule-based strategy to filter out the *hardest negatives*, i.e., the most similar samples in semantics, by considering the temporal dependencies (closeness and periodicity) within STG. In other words, we exclude these similar samples when calculating the contrastive loss. Our contributions are summarized as follows:

- We propose a novel framework termed STGCL that integrates contrastive learning with STG forecasting to embrace both accuracy and robustness. It can easily serve as a plug-in to existing spatio-temporal models.
- By fully considering the unique properties of STG, we design four types of data augmentation methods for STG data and propose to filter out the hardest negatives per anchor, leading to an extension to the contrastive loss.

- We evaluate STGCL across various types of traffic datasets and across different kinds of models (CNN-based and RNN-based). The results demonstrate the consistent improvements achieved by STGCL, with larger improvements for long-term predictions.

2 Preliminaries

2.1 Spatio-temporal Graph Forecasting

We define the sensor network as a graph $G = (\mathcal{V}, \mathcal{E}, \mathbf{A})$, where \mathcal{V} is a set of nodes (sensors) and $|\mathcal{V}| = N$, \mathcal{E} is a set of edges, and $\mathbf{A} \in \mathbb{R}^{N \times N}$ is a weighted adjacency matrix (each weight represents the proximity between nodes). The graph G has a unique feature matrix $\mathbf{X}^t \in \mathbb{R}^{N \times F}$ at each time step t , where F is the size of feature dimension and it typically consists of F' target attributes (e.g. traffic speed and flow) and other auxiliary information, such as “time of day”. Therefore, the task of STG forecasting is formulated as learning a function f , which predicts the next T steps based on historical S observations, i.e.,

$$[\mathbf{X}^{(t-S):t}, G] \xrightarrow{f} \mathbf{Y}^{t:(t+T)} \quad (1)$$

where $\mathbf{X}^{(t-S):t} \in \mathbb{R}^{S \times N \times F}$ contains feature information from time $t - S$ to t (excluding the right endpoint), and $\mathbf{Y}^{t:(t+T)} \in \mathbb{R}^{T \times N \times F'}$ is the T -step ahead predictions.

2.2 Graph Contrastive Learning

The goal of graph contrastive representation learning is to learn a GNN encoder that can extract useful graph-level representations from the inputs. A typical graph contrastive learning framework (e.g. GraphCL (You et al. 2020)) works as follows. For an input graph, stochastic data augmentation methods are applied to generate two correlated views, which are then forwarded through a GNN encoder network and a readout function to obtain two high-level graph representations. A non-linear transformation named the “projection head” further maps the graph representations to another latent space, where the contrastive loss is computed.

During training, a batch of M graphs are sampled and processed through the above procedure, resulting in a total of $2M$ representations. Let $\mathbf{z}_{n,i}, \mathbf{z}_{n,j}$ denote the two correlated views from the n th graph in a batch and $\text{sim}(\mathbf{z}_{n,i}, \mathbf{z}_{n,j})$ denote the cosine similarity between them. The contrastive loss applied in GraphCL (You et al. 2020) is a variant of the InfoNCE loss (Oord, Li, and Vinyals 2018; Chen et al. 2020), which is defined as:

$$\mathcal{L}_n = -\log \frac{\exp(\text{sim}(\mathbf{z}_{n,i}, \mathbf{z}_{n,j})/\tau)}{\sum_{n'=1, n' \neq n}^M \exp(\text{sim}(\mathbf{z}_{n,i}, \mathbf{z}_{n',j})/\tau)} \quad (2)$$

where τ denotes the temperature parameter and a total of $M - 1$ negative samples are incorporated for the n th graph. The final loss is calculated across all the graph samples in the batch.

To use the pretrained model for downstream tasks, such as graph classification, a linear classifier is trained using cross-entropy loss on top of the GNN encoder, which may be frozen (linear evaluation) or unfrozen (fine-tuning). The projection head is discarded at inference time.

3 Methodology

3.1 Overview

In this paper, we propose a novel framework STGCL that enhances STG forecasting with contrastive learning and makes full use of the unique characteristics of STG data. Our goal is to encourage the spatio-temporal summaries obtained from the encoder to be invariant to disturbance and to be discriminative to distinguish different samples' spatio-temporal patterns. These will help to improve performance and strengthen the model's robustness. The pipeline of STGCL is depicted as follows (also see Figure 2).

Firstly, a *data augmentation* module is leveraged to transform a sample $\mathcal{G} = [\mathbf{X}^{(t-S):t}; G]$ to its correlated view \mathcal{G}' . The applied augmentations are described in Section 3.2. Then we use a *spatio-temporal encoder* to map both the original input and the augmented input to high-level representations $\mathbf{H}, \mathbf{H}' \in \mathbb{R}^{N \times D}$, where D denotes the size of the hidden dimension. The temporal dimension is eliminated because the knowledge has been encoded into the representations. Subsequently, the representations are flowed into the following two branches.

- A *predictive branch* that feeds the representation \mathbf{H} through a *spatio-temporal decoder* to forecast the future steps. The predictions of the decoder $\hat{\mathbf{Y}}^{t:(t+T)}$ are used to compute the forecasting loss with the ground truth.
- A *contrastive branch* that takes both \mathbf{H} and \mathbf{H}' as inputs to conduct the auxiliary contrastive task. Specifically, we utilize a summation function as a readout function to obtain the spatio-temporal summaries $\mathbf{s}, \mathbf{s}' \in \mathbb{R}^D$ of the input data. We further map the summaries to the latent space $\mathbf{z}, \mathbf{z}' \in \mathbb{R}^D$ by a projection head. The applied projection head has two linear layers, where the first layer is followed by batch normalization and rectified linear units. Finally, a contrastive loss is used to maximize the similarities between \mathbf{z} and \mathbf{z}' (a positive pair), and minimize the similarities between \mathbf{z} and other samples' augmented views (negative pairs). Here, we propose to avoid forming negative pairs between the most semantically similar samples by a negative filtering operation.

3.2 Data Augmentation

Data augmentation is a crucial component of the contrastive learning framework. It helps to build semantically similar pairs and has a great impact on the quality of the learned representations (Chen et al. 2020). Several augmentation methods on graphs have been proposed in (You et al. 2020; Zeng and Xie 2021), such as edge perturbation and subgraph sampling. However, they are originally designed for conventional graphs, which is not the case for STG. For example, they do not consider the temporal correlations.

In this work, we propose four types of data augmentation methods for STG, which disturb data in the aspects of graph structure, time domain, and frequency domain, thus making the learned representation less sensitive to changes of graph structure or signals. Note that we denote $\mathbf{X}^{(t-S):t} \in \mathbb{R}^{S \times N}$ in this section, because only the target attributes (e.g. traffic speed) are modified and the remaining input attributes are untouched. We give the details of each method as follows.

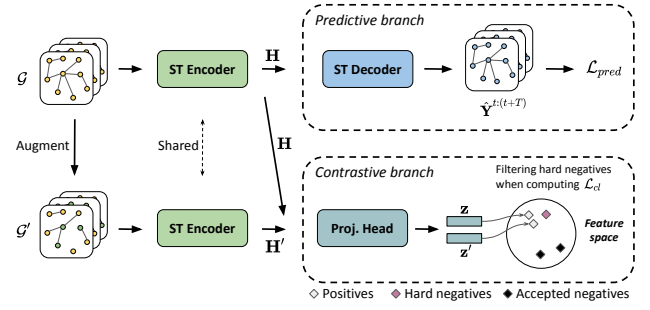


Figure 2: Overview of the Spatio-Temporal Graph Contrastive Learning framework (STGCL). The missing edges and green nodes in \mathcal{G}'_i indicate the disturbance on graph structure and signals, respectively.

Edge masking Edge perturbation (You et al. 2020) suggests either add or delete a certain ratio of edges to/from an unweighted graph. However, it is an awkward fit for the weighted adjacency matrix used in STG forecasting, since assigning proper weights to the added edges is difficult. Therefore, we make a small revision by masking (deleting) entries of the adjacency matrix to disturb the graph structure. Each entry of the augmented matrix \mathbf{A}' is given by:

$$\mathbf{A}'_{ij} = \begin{cases} \mathbf{A}_{ij}, & \text{if } \mathbf{M}_{ij} \geq r_{em} \\ 0, & \text{otherwise} \end{cases} \quad (3)$$

where $\mathbf{M} \sim U(0, 1)$ is a random matrix and r_{em} is tunable. We share the augmented matrix across the samples within a batch for efficiency. This method is applicable for both predefined and adaptive adjacency matrix (Wu et al. 2019).

Input masking As mentioned before, there are often some missing values in STG data. To strengthen the model robustness to this factor, we simulate this process by masking entries of the original input feature matrix. Each entry of the augmented feature matrix $\mathbf{P}^{(t-S):t}$ is generated by:

$$\mathbf{P}^{(t-S):t}_{ij} = \begin{cases} \mathbf{X}^{(t-S):t}_{ij}, & \text{if } \mathbf{M}_{ij} \geq r_{im} \\ 0, & \text{otherwise} \end{cases} \quad (4)$$

where $\mathbf{M} \sim U(0, 1)$ is a random matrix and r_{im} is tunable.

Temporal shifting STG data derive from nature and evolve over time continuously. However, they can only be recorded by sensors in a discrete manner, e.g., 5 minutes per reading. Motivated by this, we shift the data along the time axis to exploit the intermediate status between two consecutive time steps (see Figure 3). We implement this idea by linearly interpolating between consecutive samples. Formally,

$$\mathbf{P}^{(t-S):t} = \alpha \mathbf{X}^{(t-S):t} + (1 - \alpha) \mathbf{X}^{(t-S+1):(t+1)} \quad (5)$$

where α is generated within the distribution $U(r_{ts}, 1)$ every epoch and r_{ts} is adjustable. This method is sample-specific, which means different samples have their unique α . Meanwhile, our operation can be linked to the mixup augmentation (Zhang et al. 2017). The major difference is that we conduct weighted averaging between two successive time steps to ensure interpolation accuracy.

Input smoothing To defeat the data noise in STG, this method smooths the inputs by scaling high-frequency entries in the frequency domain (see Figure 3). Specifically, we first concatenate histories with future values (both are available during training) to enlarge the length of the time series sequence to $L = S + T$, and obtain $\mathbf{X}^{(t-S):(t+T)} \in \mathbb{R}^{L \times N}$. Then we apply Discrete Cosine Transform (DCT) to convert the sequence of each node from the time domain to the frequency domain. We keep the low frequency E_{is} entries unchanged and scale the high frequency $L - E_{is}$ entries by the following steps: 1) We generate a random matrix $\mathbf{M} \in \mathbb{R}^{(L-E_{is}) \times N}$, which satisfies $\mathbf{M} \sim U(r_{is}, 1)$ and r_{is} is adjustable. 2) We leverage normalized adjacency matrix $\tilde{\mathbf{A}}$ to smooth the generated matrix by $\mathbf{M} = \mathbf{M}\tilde{\mathbf{A}}^2$. The intuition is that neighboring sensors should have similar scaling ranges and multiplying two steps of $\tilde{\mathbf{A}}$ should be sufficient to smooth the data. This step can be omitted when the adjacency matrix is not available. 3) We element-wise multiply the random numbers with the original $L - E_{is}$ entries. Finally, we use Inverse DCT (IDCT) to convert data back to the time domain.

3.3 ST Encoder & Decoder

One of the major advantages of our framework is its generality, i.e., it can be incorporated into most existing models for STG forecasting. Among them, there are two mainstreams: CNN-based and RNN-based methods. Here, we briefly introduce their architectures. For the form of the encoder, CNN-based methods usually apply temporal convolutions and graph convolutions sequentially (Wu et al. 2019) or synchronously (Song et al. 2020) to capture spatio-temporal dependencies. The widely applied form of temporal convolution is the dilated casual convolution (Yu and Koltun 2016), which enjoys an exponential growth of the receptive field by increasing the layer depth. While in RNN-based methods, graph convolution is integrated with recurrent neural networks. For example, Li et al. (2018) replace the matrix multiplications in gated recurrent unit with a diffusion convolution. For the form of the decoder, CNN-based models often apply several linear layers to map high dimensional representations to low dimensional outputs. In RNN-based models, they either employ a feed-forward network or a recurrent neural network for generating the final predictions.

3.4 Dual-Task Training

Negative filtering The samples built in STG forecasting have temporal correlations to each other, such as closeness and periodicity (Zhang, Zheng, and Qi 2017). For example, Figure 4 illustrates the average traffic speed of different time steps on the PEMS-BAY dataset (Li et al. 2018). We can observe that the pattern from 6 am to 7 am on Monday is similar to that day from 7 am to 8 am (closeness), and also similar to the same time on Tuesday (daily periodic) and next Monday (weekly periodic). Hence, temporally close samples (regardless of the day) are likely to have similar spatio-temporal representations in the latent space. If we form negative pairs by using these semantically similar samples (i.e., hard negative samples) and push apart their representations,

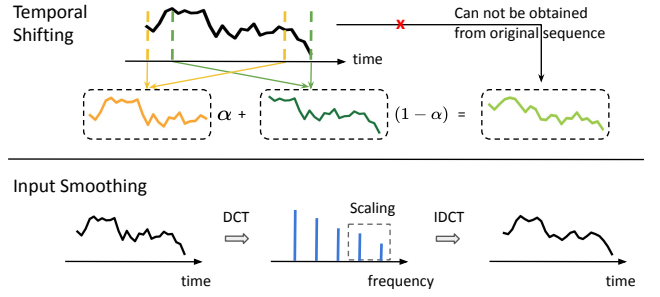


Figure 3: Sketch of temporal shifting and input smoothing.

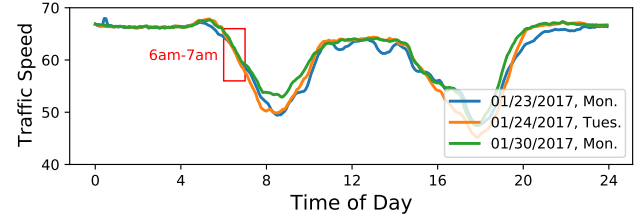


Figure 4: Example of temporal correlations in STG data.

it may break the semantic structure and worsen performance.

Therefore, we propose a rule-based strategy that leverages the attribute “time of day” in the input to filter out the hardest negatives per anchor. In this paper, due to the lack of semantic labels in the regression task, we define the hardest negatives using a threshold r_f . Specifically, denoting the starting “time of day” of an anchor as t_i , we can obtain a set of acceptable negatives $\{\mathbf{z}_i''\}$ within a batch, where each sample’s starting “time of day” t satisfies $|t - t_i| > r_f$, and r_f is a controllable threshold. We empirically find that the choice of r_f is of great importance to the quality of learned representations. For instance, using a very large r_f will significantly reduce the number of negative samples, which may impair the contrastive task. For more details, please see Section 4.4.

Loss function During training, a batch of M samples is randomly sampled and processed through the procedure in Section 3.1. Let $\text{sim}(\mathbf{z}_i, \mathbf{z}_i') = \mathbf{z}_i^T \mathbf{z}_i' / \|\mathbf{z}_i\| \|\mathbf{z}_i'\|$ denote the cosine distance between vectors and τ denote the temperature parameter, our filtering operation extends the contrastive loss in Eq. 2 to the form:

$$\mathcal{L}_{cl} = \frac{1}{M} \sum_{i=1}^M -\log \frac{\exp(\text{sim}(\mathbf{z}_i, \mathbf{z}_i')/\tau)}{\sum_{\mathbf{z}_j \in \{\mathbf{z}_i''\}} \exp(\text{sim}(\mathbf{z}_i, \mathbf{z}_j)/\tau)} \quad (6)$$

If r_f is set to zero, all samples in a batch are used to form the negative pairs with the anchor and Eq. 6 degrades to Eq. 2. We use the mean absolute error (MAE) as the loss function of the main (prediction) task, which is defined in Eq. 7. The final form of the loss function in STGCL is given in Eq. 8, where λ is a trade-off between two terms.

$$\mathcal{L}_{pred} = \frac{1}{M} \sum_{i=1}^M |\hat{\mathbf{Y}}_i^{t:(t+T)} - \mathbf{Y}_i^{t:(t+T)}| \quad (7)$$

$$\mathcal{L} = \mathcal{L}_{pred} + \lambda \mathcal{L}_{cl} \quad (8)$$

4 Experiments

4.1 Experimental Setup

Datasets We evaluate the performance of STGCL on three real-world traffic datasets: PEMS-BAY (Li et al. 2018), PEMS-04 (Guo et al. 2019), and PEMS-08 (Guo et al. 2019). The datasets are collected by the Caltrans Performance Measurement System (Chen et al. 2001). There are three kinds of traffic measurements contained in the raw data, including traffic flow, average speed, and average occupancy. These traffic readings are aggregated into 5-minute windows, resulting in 288 data points per day. We use the 12-step historical data to predict the next 12 steps. Z-score normalization is applied to the input data. The adjacency matrix is constructed by road network distance with a thresholded Gaussian kernel (Shuman et al. 2013). The datasets are divided into three parts for training, validation, and test with a ratio of 7:1:2 on PEMS-BAY, and 6:2:2 on PEMS-04 and PEMS-08. The dataset statistics are provided in Table 1.

Table 1: Dataset statistics. See more details in Appendix.

Datasets	#Nodes	#Edges	#Time steps
PEMS-BAY	325	2,369	52,116
PEMS-04	307	340	16,992
PEMS-08	170	295	17,856

Base Models We use four base models that belong to the following two classes: CNN-based models (GWN, MT-GNN) and RNN-based models (DCRNN, AGCRN).

- **GWN**: Graph WaveNet combines adaptive adjacency matrix with graph convolution and uses dilated casual convolution (Wu et al. 2019).
- **MTGNN**: A GNN framework designed for multivariate time series forecasting. It proposes a graph learning module and applies graph convolution with mix-hop propagation and dilated inception layer (Wu et al. 2020).
- **DCRNN**: Diffusion Convolution Recurrent Neural Network, which integrates diffusion convolution into RNNs in an encoder-decoder manner (Li et al. 2018).
- **AGCRN**: This approach develops two adaptive modules to enhance graph convolution and combines them into RNNs (Bai et al. 2020).

Implementation Details We use PyTorch to implement all the base models and our method. All the experiments in this section are repeated 5 times with different seeds. We basically employ the default settings of base models from their source code, such as model configurations, batch size, optimizer, learning rate, and gradient clipping. The settings of STGCL follow the same as in base models’ implementation, except that we don’t apply weight decay, as this will introduce another term in the loss function. The maximum number of epochs in the experiments is fixed to 100. The temperature τ is set to 0.1 after tuning within the range of $\{0.05, 0.1, 0.15, 0.2, 0.25\}$. We adopt three kinds of metrics to evaluate the model performance, including mean absolute error (MAE), root mean squared error (RMSE), and mean

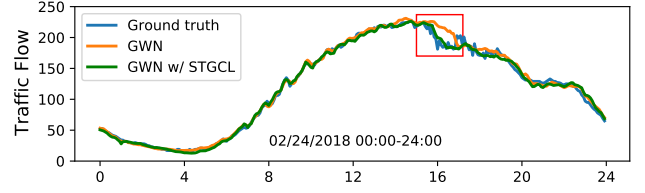


Figure 5: Visualization of 60 minutes-ahead predictions on a snapshot of the PEMS-04 test set.

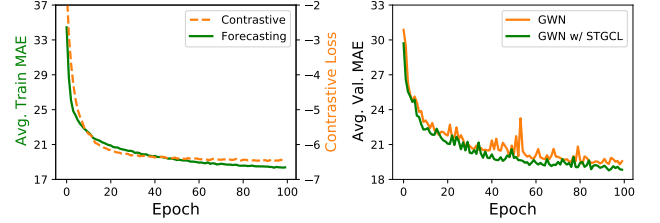


Figure 6: The left part shows the training curve of forecasting MAE and contrastive loss by using GWN w/ STGCL on PEMS-04. The right part shows the validation MAE of GWN w/ STGCL against pure GWN on PEMS-04.

absolute percentage error (MAPE). More details about the experimental settings can be found in Appendix.

4.2 Performance Comparison

Table 2 presents the test MAE results of the average values over all predicted horizons and three specific horizons (15, 30, and 60 minutes). The complete table that include MAE, RMSE, MAPE, and the specific settings for the reported results are provided in Appendix. Our results show that STGCL achieves consistent improvements across all base models on all datasets, which verifies the effectiveness of using contrastive loss and suggests that STGCL is model-agnostic, i.e., it can be applied to both CNN-based and RNN-based model architectures. Note that particularly on the best performing models such as GWN and MTGNN, the improvements from STGCL are in many cases several times the standard deviation, especially on PEMS-04 and PEMS-08, suggesting that they are statistically significant. It is also worth mentioning that some of the improvements derived from STGCL are even larger than using an advanced model. For instance, GWN obtains an average MAE of 19.33 on PEMS-04, while the MAE is reduced to 18.88 after applying STGCL, better than MTGNN (MAE=19.09). In addition, the standard deviation of STGCL is generally smaller than that of the base model, which indicates that STGCL can provide additional stability.

Another important observation in Table 2 is that STGCL achieves larger improvements for long-term predictions, e.g., at the 60-minute horizon with bold fonts. To investigate it, we use GWN as the base model and randomly select a sensor (#200) from PEMS-04 for a case study. Figure 5 visualizes the 60 minutes-ahead prediction results against the ground truth on a snapshot of the test data. It can be seen that

Table 2: Test MAE results of the base models and our method on PEMS-BAY, PEMS-04, and PEMS-08. min: minutes.

Methods	PEMS-BAY				PEMS-04				PEMS-08			
	Avg.	15 min	30 min	60 min	Avg.	15 min	30 min	60 min	Avg.	15 min	30 min	60 min
GWN	1.59±.01	1.31±.00	1.64±.01	1.97±.03	19.33±.11	18.20±.09	19.32±.13	21.10±.18	14.78±.03	13.80±.05	14.75±.04	16.39±.09
w/ STGCL	1.54±.00	1.29±.00	1.61±.00	1.88±.01	18.88±.04	17.93±.04	18.87±.04	20.40±.09	14.61±.03	13.67±.04	14.61±.03	16.09±.05
MTGNN	1.59±.01	1.34±.02	1.66±.01	1.94±.02	19.09±.04	18.32±.05	19.10±.05	20.39±.09	15.34±.09	14.36±.06	15.34±.10	16.91±.16
w/ STGCL	1.56±.01	1.32±.00	1.63±.01	1.89±.01	18.68±.04	17.99±.03	18.72±.05	19.88±.07	14.88±.04	14.04±.05	14.90±.05	16.23±.08
DCRNN	1.66±.05	1.34±.03	1.71±.05	2.09±.08	22.70±.21	19.99±.11	22.40±.19	27.15±.35	17.11±.25	15.23±.15	16.98±.25	20.27±.41
w/ STGCL	1.63±.00	1.32±.00	1.68±.00	2.05±.00	22.34±.13	19.82±.08	22.07±.12	26.51±.21	17.01±.20	15.19±.11	16.89±.19	20.09±.34
AGCRN	1.63±.01	1.37±.00	1.69±.01	1.99±.01	19.39±.03	18.53±.03	19.43±.06	20.72±.03	15.79±.06	14.58±.07	15.71±.07	17.82±.11
w/ STGCL	1.61±.01	1.35±.00	1.67±.01	1.96±.01	19.13±.05	18.31±.04	19.17±.06	20.39±.03	15.62±.07	14.51±.05	15.56±.06	17.51±.10

Table 3: Effects of λ on PEMS-04 and PEMS-08.

Lambda	PEMS-04		PEMS-08	
	GWN	AGCRN	GWN	AGCRN
0.01	18.91±0.14	19.33±0.09	14.71±0.02	15.82±0.06
0.05	18.91±0.06	19.30±0.11	14.61±0.03	15.67±0.04
0.1	18.91±0.06	19.19±0.04	14.64±0.06	15.62±0.07
0.5	18.88±0.04	19.16±0.04	14.69±0.06	15.76±0.05
1.0	18.95±0.11	19.29±0.11	14.72±0.05	15.89±0.06

GWN w/ STGCL outperforms the counterpart, especially at the sudden change (see the red rectangle). A plausible explanation to this is that STGCL has learned discriminative representations by receiving signals from contrastive task during training, hence it can successfully distinguish some distinct patterns (like sudden changes).

Besides, we plot the learning curves of the two losses (\mathcal{L}_{pred} and \mathcal{L}_{cl}) in Figure 6 (left-hand side) to further verify the learning of the dual tasks. The reason why the contrastive loss is less than 0 is that the denominator of the contrastive loss does not contain the numerator, thus their ratio can be greater than 1. While on the right-hand side of the figure, we plot the trends of the validation MAE. It is clear that STGCL achieves better performance and is more stable than the pure GWN model. Next, we select one CNN-based model (GWN) and one RNN-based model (AGCRN) as representatives to show the effects of each component.

4.3 Effects of Data Augmentation

We show the effects of different augmentation methods by tuning the hyper-parameter related to that method in Figure 7. We highlight the best performance achieved by each model on each augmentation method in the figure. For input smoothing, the fixed entries $E_{i,s}$ is set to 20 after tuning within the range of $\{16, 18, 20, 22\}$.

From the figures, we have the following observations: 1) all the proposed data augmentations can successfully improve performance over the base models. 2) The best performance achieved by each augmentation method has little difference, though the semantics of each method is different (e.g., temporal shifting and input smoothing are performed in the time and frequency domain, respectively). This indicates that STGCL is not sensitive to augmentation semantics. 3) Input masking is significantly affected by the disturbance magnitude, while other augmentation methods are rel-

Table 4: Effects of threshold r_f on PEMS-04 and PEMS-08.

Filtering threshold	PEMS-04		PEMS-08	
	GWN	AGCRN	GWN	AGCRN
0 min	19.00±0.07	19.26±0.04	14.67±0.03	15.73±0.06
30 min	18.93±0.03	19.13±0.05	14.63±0.02	15.70±0.13
60 min	18.88±0.04	19.16±0.04	14.61±0.03	15.62±0.07
90 min	18.93±0.07	19.28±0.03	14.65±0.04	15.76±0.08
120 min	18.94±0.09	19.34±0.11	14.68±0.07	15.75±0.10

atively stable and do not have an obvious trend. The reason could be that masking a certain fraction of entries to zero disturbs input a lot, but the disturbance injected by other augmentations is considered reasonable by the models. 4) Input masking with a 1% ratio achieves most of the best performance across the applied models and datasets. We thereby suggest using this setting in other datasets for initiatives.

4.4 Effects of Contrastive Loss

We show the effects of loss term trade-off parameter λ in Table 3 and the filtering threshold r_f in Table 4. Input masking with a 1% ratio is used as the default augmentation setting. The results show that tuning λ within $\{0.01, 0.05, 0.1, 0.5, 1.0\}$ is sufficient to find the best value and the PEMS-04 dataset prefers a larger λ than that on the PEMS-08 dataset.

For the negative filtering operation, we show that the filtering threshold r_f works best when set to 30 or 60 minutes, which demonstrates the effectiveness of our simple solution. We also notice that when r_f is set to 120 minutes, some results are worse than when r_f is set to 0. The reason is that the threshold of 120 minutes filters out too many negatives and the contrastive task becomes too easy, hence the model may not be able to learn useful discrimination knowledge. One insight we can draw from the experimental results is that by filtering out the hardest negative samples (the most semantically similar samples), we can help the contrastive loss focus on the *true* negative samples. On the other hand, filtering too many negatives makes the contrastive task meaningless and leads to performance degradation.

Our negative filtering operation is also more efficient in measuring the similarity of two time series sequences than existing methods such as dynamic time warping (Berndt and Clifford 1994) or Pearson correlation coefficient. The reason is that our method only needs to compare the starting time of each sample and does not involve other computations.

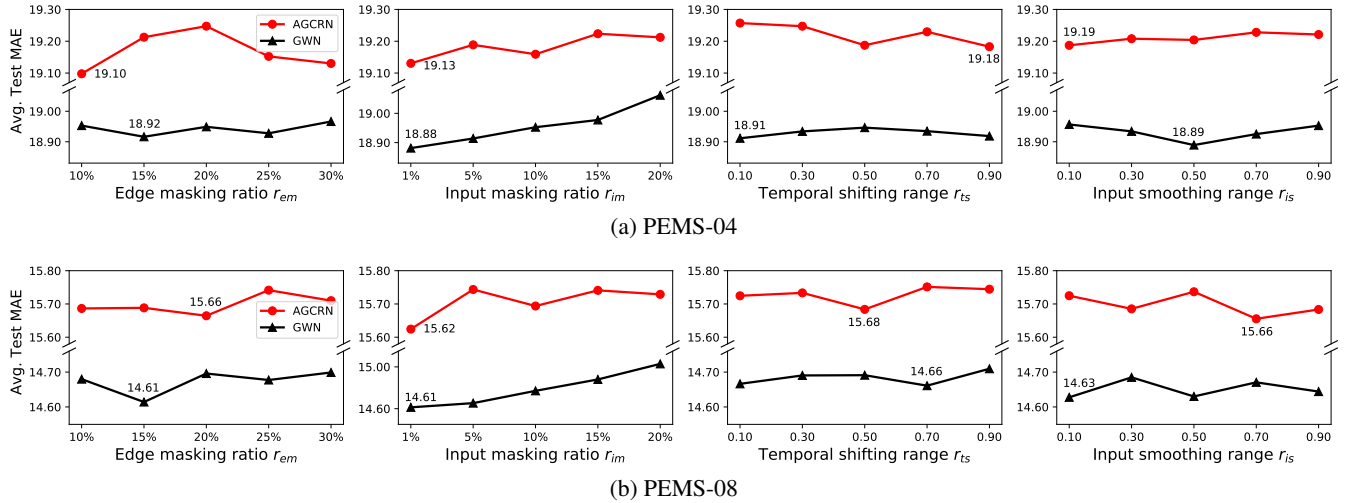


Figure 7: Effects of different augmentation methods on the PEMS-04 and PEMS-08 datasets.

5 Related Work

5.1 Deep Learning for Spatio-Temporal Graphs

STG forecasting is a typical problem in smart city efforts, facilitating a wide range of applications, such as traffic forecasting and air quality prediction. Recently, spatio-temporal graph neural networks have become the dominant class for modeling STG. They either integrate graph convolutions with CNNs or RNNs to capture the spatial and temporal dependencies within STG. As a pioneering work, DCRNN (Li et al. 2018) considers traffic flow as a diffusion process and proposes a novel diffusion convolution to capture spatial dependencies. To improve training speed, GWN (Wu et al. 2019) adopts a complete convolutional structure, which combines graph convolution with dilated casual convolution operation. It also proposes an adaptive adjacency matrix as a complement to the predefined one. In addition, GeoMAN (Liang et al. 2018) and ASTGCN (Guo et al. 2019) introduce attention mechanisms on both spatial and temporal dimensions to capture the dynamics of spatio-temporal correlations. The recent developments in this field show the following trends: make the adjacency matrix fully learnable (Bai et al. 2020), and developing modules to jointly capture spatial and temporal dependencies (Song et al. 2020).

5.2 Contrastive Learning on Graphs

Recently, contrastive representation learning approaches on graphs have attracted significant attention. According to the taxonomy from a recent survey (Liu et al. 2021), existing methods can be divided into cross-scale contrasting and same-scale contrasting.

Cross-scale contrasting refers to the scenario that the contrastive elements are in different scales. For example, a representative work named DGI (Velickovic et al. 2019) contrasts between the node and graph-level representations via mutual information (MI) maximization, thus gaining benefits from flowing global information to local representations. MVGRL (Hassani and Khasahmadi 2020) further suggests a

multi-view contrasting by using a diffused graph as a global view of the original graph, after which the MI is maximized in a cross-view and cross-scale manner.

For same-scale contrasting, graph elements are contrasting in an equal scale, such as node-node and graph-graph contrasting. Regarding the definition of positive/negative pairs, the approaches can be further divided into context-based and augmentation-based. The context-based methods generally utilize random walks to obtain positive samples. Our work lies in the scope of augmentation-based methods, where the positive samples are generated by disturbance on nodes or edges. A representative work GraphCL (You et al. 2020) adopts four graph augmentations to form positive pairs and contrasts at graph level. GCA (Zhu et al. 2021) works at the node level and performs augmentations that are adaptive to the graph structure and attributes.

6 Conclusion and Future Work

This study explores the potential of utilizing contrastive learning techniques to improve STG forecasting performance. In particular, we have presented STGCL, a novel and model-agnostic framework that enhances the forecasting task with a supplementary contrastive task. Four STG-specific augmentations that differ from the methods on the general graphs are devised to construct positive pairs. We also propose a rule-based strategy to alleviate an inherent shortcoming of the unsupervised contrastive method, i.e., ignoring the sample’s semantic similarity. The extensive experiments on four state-of-the-art models and three real-world datasets have demonstrated the superiority of STGCL. Besides, we have noticed that each component of STGCL still has space to improve. In the future, we plan to leverage adaptive data augmentation techniques to identify the importance of edges/nodes, thus treating them differently when generating augmented views. Another direction is designing a learnable negative filtering method that can dynamically assign weights to hard negatives, rather in a rule-based way.

References

- Bai, L.; Yao, L.; Li, C.; Wang, X.; and Wang, C. 2020. Adaptive Graph Convolutional Recurrent Network for Traffic Forecasting. In *Proceedings of Advances in Neural Information Processing Systems*, volume 33, 17804–17815.
- Berndt, D. J.; and Clifford, J. 1994. Using dynamic time warping to find patterns in time series. In *KDD workshop*, volume 10, 359–370.
- Chen, C.; Petty, K.; Skabardonis, A.; Varaiya, P.; and Jia, Z. 2001. Freeway performance measurement system: mining loop detector data. *Transportation Research Record*, 1748: 96–102.
- Chen, T.; Kornblith, S.; Norouzi, M.; and Hinton, G. 2020. A simple framework for contrastive learning of visual representations. In *Proceedings of International conference on machine learning*, 1597–1607.
- Guo, S.; Lin, Y.; Feng, N.; Song, C.; and Wan, H. 2019. Attention based spatial-temporal graph convolutional networks for traffic flow forecasting. In *Proceedings of the AAAI Conference on Artificial Intelligence*, volume 33, 922–929.
- Hassani, K.; and Khasahmadi, A. H. 2020. Contrastive multi-view representation learning on graphs. In *Proceedings of International Conference on Machine Learning*, 4116–4126.
- Hu, Z.; Dong, Y.; Wang, K.; Chang, K.-W.; and Sun, Y. 2020. Gpt-gnn: Generative pre-training of graph neural networks. In *Proceedings of the 26th ACM SIGKDD International Conference on Knowledge Discovery & Data Mining*, 1857–1867.
- Kipf, T. N.; and Welling, M. 2017. Semi-supervised classification with graph convolutional networks. In *Proceedings of International Conference on Learning Representations*.
- Li, M.; and Zhu, Z. 2021. Spatial-Temporal Fusion Graph Neural Networks for Traffic Flow Forecasting. In *Proceedings of the AAAI Conference on Artificial Intelligence*, 4189–4196.
- Li, Y.; Yu, R.; Shahabi, C.; and Liu, Y. 2018. Diffusion convolutional recurrent neural network: Data-driven traffic forecasting. In *Proceedings of International Conference on Learning Representations*.
- Liang, Y.; Ke, S.; Zhang, J.; Yi, X.; and Zheng, Y. 2018. Geoman: Multi-level attention networks for geo-sensory time series prediction. In *Proceedings of International Joint Conference on Artificial Intelligence*, volume 2018, 3428–3434.
- Liu, Y.; Pan, S.; Jin, M.; Zhou, C.; Xia, F.; and Yu, P. S. 2021. Graph self-supervised learning: A survey. *arXiv preprint arXiv:2103.00111*.
- Oord, A. v. d.; Li, Y.; and Vinyals, O. 2018. Representation learning with contrastive predictive coding. *arXiv preprint arXiv:1807.03748*.
- Pan, Z.; Liang, Y.; Wang, W.; Yu, Y.; Zheng, Y.; and Zhang, J. 2019. Urban traffic prediction from spatio-temporal data using deep meta learning. In *Proceedings of the 25th ACM SIGKDD International Conference on Knowledge Discovery & Data Mining*, 1720–1730.
- Shuman, D. I.; Narang, S. K.; Frossard, P.; Ortega, A.; and Vandergheynst, P. 2013. The emerging field of signal processing on graphs: Extending high-dimensional data analysis to networks and other irregular domains. *IEEE signal processing magazine*, 30: 83–98.
- Song, C.; Lin, Y.; Guo, S.; and Wan, H. 2020. Spatial-temporal synchronous graph convolutional networks: A new framework for spatial-temporal network data forecasting. In *Proceedings of the AAAI Conference on Artificial Intelligence*, volume 34, 914–921.
- Veličković, P.; Cucurull, G.; Casanova, A.; Romero, A.; Lio, P.; and Bengio, Y. 2018. Graph attention networks. In *Proceedings of International Conference on Learning Representations*.
- Velickovic, P.; Fedus, W.; Hamilton, W. L.; Liò, P.; Bengio, Y.; and Hjelm, R. D. 2019. Deep Graph Infomax. In *Proceedings of International Conference on Learning Representations*.
- Wu, Z.; Pan, S.; Long, G.; Jiang, J.; Chang, X.; and Zhang, C. 2020. Connecting the dots: Multivariate time series forecasting with graph neural networks. In *Proceedings of the 26th ACM SIGKDD International Conference on Knowledge Discovery & Data Mining*, 753–763.
- Wu, Z.; Pan, S.; Long, G.; Jiang, J.; and Zhang, C. 2019. Graph wavenet for deep spatial-temporal graph modeling. In *Proceedings of International Joint Conference on Artificial Intelligence*.
- Yi, X.; Zheng, Y.; Zhang, J.; and Li, T. 2016. ST-MVL: filling missing values in geo-sensory time series data. In *Proceedings of International Joint Conference on Artificial Intelligence*.
- You, Y.; Chen, T.; Sui, Y.; Chen, T.; Wang, Z.; and Shen, Y. 2020. Graph contrastive learning with augmentations. In *Proceedings of Advances in Neural Information Processing Systems*, volume 33.
- Yu, F.; and Koltun, V. 2016. Multi-scale context aggregation by dilated convolutions. In *Proceedings of International Conference on Learning Representations*.
- Zeng, J.; and Xie, P. 2021. Contrastive self-supervised learning for graph classification. In *Proceedings of the AAAI Conference on Artificial Intelligence*.
- Zhang, H.; Cisse, M.; Dauphin, Y. N.; and Lopez-Paz, D. 2017. mixup: Beyond empirical risk minimization. In *Proceedings of International Conference on Learning Representations*.
- Zhang, J.; Zheng, Y.; and Qi, D. 2017. Deep spatio-temporal residual networks for citywide crowd flows prediction. In *Proceedings of the AAAI Conference on Artificial Intelligence*.
- Zhu, Y.; Xu, Y.; Yu, F.; Liu, Q.; Wu, S.; and Wang, L. 2021. Graph contrastive learning with adaptive augmentation. In *Proceedings of the Web Conference 2021*, 2069–2080.